

## Study of Iron Silicide Formed by Ion Beam Mixing.

Rachid Ayache<sup>1\*</sup>, A. Bouabellou<sup>2</sup>, F. Eichhorn<sup>3</sup> and F. Kermiche<sup>2</sup>

<sup>1</sup>Pharmacy Department, University of Batna, 05000 Batna, Algeria

<sup>2</sup>Laboratoire des Couches Minces et Interfaces, Université de Constantine, 025000 Constantine, Algeria

<sup>3</sup>Forschungszentrum Rossendorf, Institut für Ionenstrahlphysik und Materialforschung, Postfach 510119, D-01314 Dresden, Germany

\*Email: ayache\_r@yahoo.fr

Received: 20 Jul. 2013; Revised: 15 Nov. 2013; Accepted: 4 Dec. 2013; Published: 1 Jul. 2014

**Abstract:** Ion beam mixing has been extensively used in Metal/Silicon systems to produce the new phases. In the present study a Fe films was deposited by thermal evaporation onto p-type Si(111). The films were irradiated with 300 keV Xe<sup>+</sup> ions at room temperature (RT) and subsequently annealed. The experimental results have shown that the Xe irradiation at RT leads to the formation only of the  $\epsilon$ -FeSi phase, and after thermal annealing the Fe layer is transformed to a mixture of  $\epsilon$ -FeSi,  $\alpha$ -FeSi<sub>2</sub> and  $\beta$ -FeSi<sub>2</sub> phases. The  $\beta$ -FeSi<sub>2</sub> having a direct band gap of 0.81 eV, is demonstrated.

**Keywords:** Ion beam mixing;  $\beta$ -FeSi<sub>2</sub>; RBS; XRD; Raman spectroscopy; PL.

### 1. INTRODUCTION

The iron silicides have many phases and have been much studied for their unusual properties that cannot be explained by traditional means, and for their applications in microelectronics devices [1]. Among the iron phases,  $\beta$ -FeSi<sub>2</sub> is semiconducting with a band gap of about 0.80 eV [4-5]. It crystallizes in orthorhombic structure (space group: Cmca) [2], with lattice constants  $a=0.9865$  nm,  $b=0.7791$  nm and  $c=0.7833$  nm at room temperature [4]. Several methods have been used for the preparation of  $\beta$ -FeSi<sub>2</sub>, such as reactive deposition epitaxy [6], pulsed laser deposition (PLD) [7], ion beam assisted deposition (IBAD) [8, 9], ion beam synthesis (IBS) [10–12] and ion beam mixing (IBM) [13, 14]. The technical significance of ion beam mixing is derived from modification of macroscopic properties of materials such as adhesion of the elements at the interface, phase formation, phase stability.

In this paper we study the formation of different phases of iron silicides at the interface of the Fe/Si system by ion beam mixing using Rutherford backscattering spectrometry (RBS), X-ray diffraction (XRD), Raman spectroscopy and Photoluminescence (PL) techniques.

### 2. EXPERIMENTAL PROCEDURE

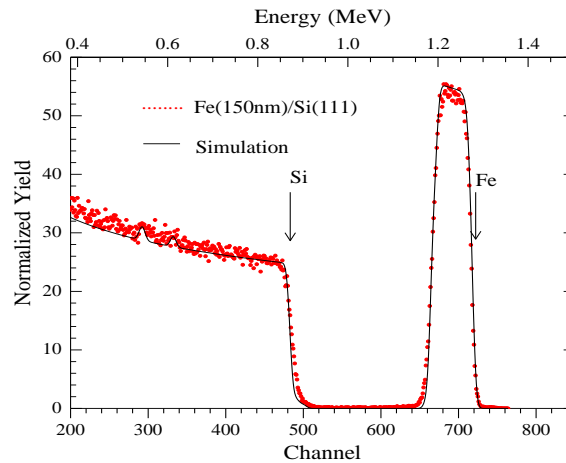
The Fe/Si samples were irradiated at room temperature (RT) with 300 keV Xe<sup>+</sup> ions, at a pressure in the range of 10<sup>-7</sup> Torr. The implanted dose was 5x10<sup>16</sup> Xe<sup>+</sup>/cm<sup>2</sup> with the ion beam current of 1.5  $\mu$ A scanned over 2x2 cm<sup>2</sup> area. Projected range of the implanted ions is RP=46.7 nm, as calculated with TRIM code [15]. After Xe-ion beam mixing, the samples were annealed in a N<sub>2</sub> atmosphere at 850°C for 1h. For analysis, a 1.7 MeV He<sup>+</sup> beam was employed. The backscattered particles were collected under normal incidence geometry using a Si-surface barrier detector with resolution of 15 keV from the full width at half maximum (FWHM), mounted in such a way that a scattering angle of 170 is defined. The experimental spectra were analyzed with the RUMP computer program [16]. The phase structure of the intermixed region was monitored via 2° grazing-angle X-ray diffraction (XRD) with rotation of samples using Cu (K $\alpha$ ) line. Raman spectra were measured at RT between 150 and 450 cm<sup>-1</sup> by means of dispersive spectrometer combined with a focal microscope. Laser light at 532.14 nm was used for excitation. PL measurements were performed at 12 K using the 632.4 nm line of an He-Ne laser. The emission was detected using a liquid nitrogen cooled Ge detector.

### 3. RESULTS & DISCUSSION

#### 3.1 Rutherford Backscattering Spectrometry (RBS)

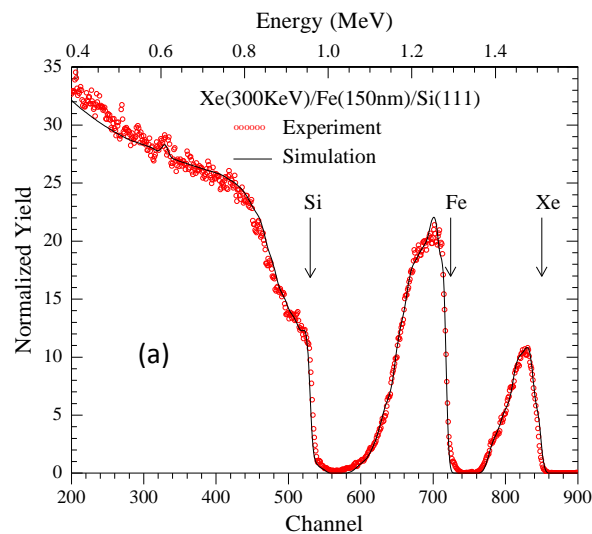
A structural analysis of mixed Fe/Si samples has shown that irradiation with 300 keV Xe<sup>+</sup> ions induces a rapid intermixing of the Fe and Si components. However, ion mixing was not efficient enough to provide complete transformation of the deposited Fe layer to desired iron disilicide. For this reason, the irradiated samples were annealed at 850°C for 1h.

Figure 1 shows a typical 1.7 MeV RBS energy spectrum backscattered for the as-deposited sample. The solid curve represents the corresponding simulation generated using Rump computer program. The thickness of the film was estimated to 150 nm, as can be seen at the low and high energy edge of the spectrum corresponding to Si and Fe signal, respectively. The boundary between the pure iron film and the silicon substrate is clearly divided, this means that the intermixture does not occur in this condition. Also the presence of oxygen and carbon impurities were found.



**Figure 1: RBS spectrum for the as-deposited samples.**

The RBS spectrum of ~150 nm thickness iron layer deposited on Si (111) irradiated at RT with 300 keV Xe<sup>+</sup> ions to a fluence of 5x10<sup>16</sup> Xe<sup>+</sup>/cm<sup>2</sup> is shown in Figure 2a. It is clear (Fig.2a) that the ion irradiation induces intermixing at Fe/Si interface. The RUMP simulation shows the formation of only iron monosilicide (FeSi), these results agree well with those of the XRD. The Figure 2b illustrates the RBS spectrum of the as-implanted and annealed sample in nitrogen atmosphere at 850°C for 1h. The intermixed layer was observed and the mean iron silicides were formed, such as FeSi and FeSi<sub>2</sub>. From the obtained spectrum, we can note the presence of carbon and oxygen as contaminants.



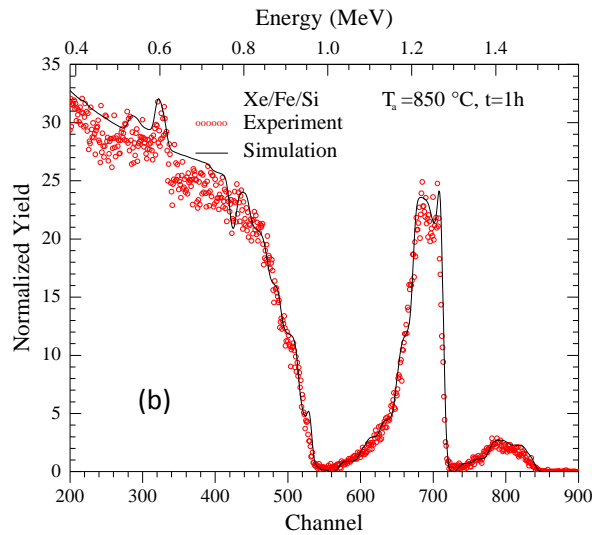


**Figure 2:** (a) RBS spectra for the as-implanted samples.  
(b) RBS spectra for the annealed samples.

### 3.2 X-ray Diffraction Characterization

Figure 3 shows the diffractograms of the as-implanted and annealed samples. It is clear that only the main diffraction peaks appear from the polycrystalline metallic  $\square$ -FeSi phase in the as-implanted sample. The formation of the  $\square$ -FeSi phase in Fe crystals with a random orientation for their part maybe the reason for it; moreover, since the height of the XRD peak mainly depends on the amount of  $\square$ -FeSi in the surface layers, it is suggested that the amount of  $\square$ -FeSi is the largest for the sample irradiated at RT.

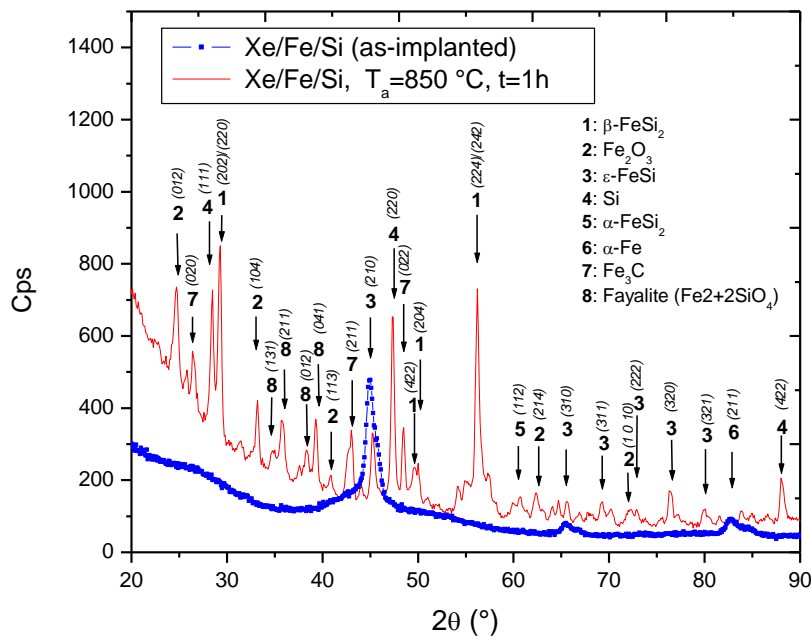


**Figure 3:** XRD patterns of the as-implanted and annealed samples.

Superimposed patterns of  $\alpha$ -FeSi<sub>2</sub>,  $\beta$ -FeSi<sub>2</sub>,  $\square$ -FeSi and Fayalite (Fe<sub>2</sub>+2SiO<sub>4</sub>) are found in the annealed sample. It is apparent that  $\beta$ -FeSi<sub>2</sub> ( $\beta$ -FeSi<sub>2</sub> (2 0 2)/(2 2 0) and  $\beta$ -FeSi<sub>2</sub>(224)/(242)) crystallites are dominant in amount than other phases. The formation of  $\square$ -FeSi<sub>2</sub> is due to the atomic rearrangement induced during defects relaxation in the annealing process or the increase in the supply

of Si atoms to the growth front of  $\alpha$ -FeSi<sub>2</sub> by enhanced diffusion of Si atoms. The iron oxide hematite Fe<sub>2</sub>O<sub>3</sub> and the carbide Fe<sub>3</sub>C were identified.

### 3.3 Raman Spectroscopy

The Raman spectrum of the annealed sample is shown in Figure 4. This figure shows peaks at 177.4, 194.3, 201.7, 248.8, 299, and 304.5 cm<sup>-1</sup> which are in good agreement with previously published data [17, 18]. The most intense peaks at 194.3 and 248.8 cm<sup>-1</sup> correspond to the Fe-Si vibrational modes [19], this is comparable to the values reported in the literature for bulk  $\alpha$ -FeSi<sub>2</sub> crystals.

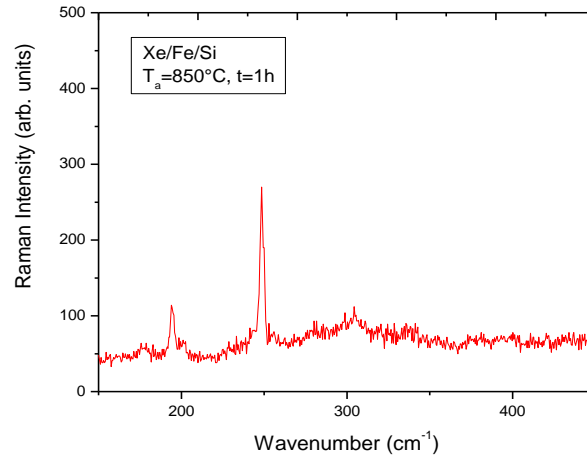


**Figure 4: Raman scattering spectrum at RT for the annealed samples.**

The additional weak peak at 299 cm<sup>-1</sup> present in the Raman spectra of  $\alpha$ -FeSi<sub>2</sub>/Si samples is attributed to the LA phonon of the silicon matrix. All experimental signals for  $\alpha$ -FeSi<sub>2</sub> are slightly shifted toward lower energies compared to those obtained theoretically [19]. This shift may be explained by the stress caused during the Xe ions irradiation and the heat treatment or due to crystalline defects of  $\alpha$ -FeSi<sub>2</sub>.

### 3.4 Photoluminescence (PL)

The PL spectrum measured at 12 K for samples annealed at 850 °C for 1h is shown in Figure 5. The main feature is an intense peak at 0.81 eV with a line width of approximately 4.8 meV. We assign this peak to optical radiative transitions intrinsic to  $\alpha$ -FeSi<sub>2</sub>. This light emission, at the wavelength of 1520.75 nm, corresponds to the band gap energy of  $\alpha$ -FeSi<sub>2</sub>. The peak, the position of which coincides with that of the well known D1 line emission (0.81 eV) at high temperature due to the dislocations in silicon matrix [20], in our case comes from  $\alpha$ -FeSi<sub>2</sub> phase because this line disappears in the non-implanted area, as already reported [21].

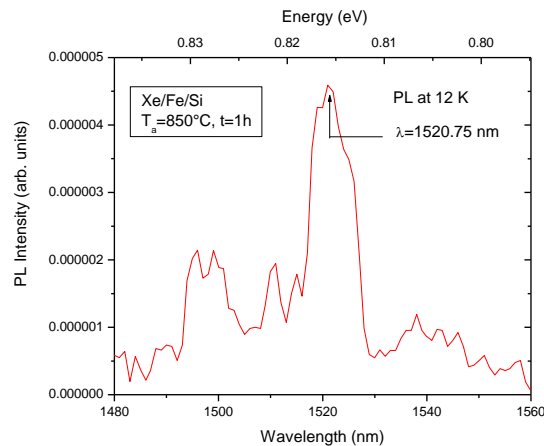


**Figure 5: PL spectrum at 12 K of the annealed samples.**

#### 4. CONCLUSION

Ion beam mixing at RT of Fe(150 nm)/Si(111) system with 300 keV Xe<sup>+</sup> with a dose of 5 x 10<sup>16</sup> Xe<sup>+</sup>/cm<sup>2</sup>, followed by annealing at 850 °C for 1h allows the formation of □-FeSi, □-FeSi<sub>2</sub> and □-FeSi<sub>2</sub> iron silicides. The shift in Raman signals may be explained by the stress caused during the implantation and the heat treatment or due to crystalline defects of □-FeSi<sub>2</sub>. In measurements, the intense PL peak observed at 0.81 eV is assigned to optical radiative transitions intrinsic to □-FeSi<sub>2</sub> silicide. No PL emission was observed for the as-implanted samples.

#### REFERENCES

- [1] A. H. Reader, A.H. van Ommen, P.J.W.Weijts, R. A. M. Wolters and D. J. Oostra, Rep. Prog. Phys. 56, 1397 (1992).
- [2] Y. Dusausoy, J. Protas, R. Wandji, and B. Roques, Acta Crystallogr. B 27, 1209 (1971).
- [3] J.E. Mahan, V. Le Thanh, J. Chevrier, I. Berbezier, and J. Derrien, J. Appl. Phys. 74, 1747 (1993).
- [4] M. C. Bost and J. E. Mahan, J. Appl. Phys. 74, 1138 (1993).
- [5] B. Schuller, R. Carius and S. Mantl, J. Appl. Phys. 94, 207 (2003).
- [6] I. Berbezier, J. L. Regolini, and C. D. Anterrosches, Microsc. Microanal. Microstruct. 4, 5 (1993).
- [7] Y. Tsuyoshi, N. Tatsuya, and N. Kunihiro, Thin Solid Films 38,1236 (2001).
- [8] A. Terrasi, S. Ravesi, C. Spinella, M. G. Grimaldi, and A. La Mantra, Thin Solid Films 188, 241 (1994).
- [9] N. P. Baradas, D. Panknin, E. Wiesser, B. Schmidt, M. Betzel, A. Mucklich, and W. Skorupa, Nucl. Instr. and Meth. B 127–128, 316 (1997).
- [10] D. Gerthsen, K. Radermacher, Ch. Deiker, and S. Mantl, J. Appl. Phys. 71, 3788 (1992).
- [11] D. J. Oostra, C.W.T. Bulle-Lieuwma, D. E. W. Vandenhoudt, F. Felten, J. C. Jans, J. Appl. Phys. 74, 4347 (1993).
- [12] Z.Q. Liu, J.Y. Feng, W.Z. Li, Nucl. Instr. and Meth. B 197, 67(2002).
- [13] M. Milosavljevic, S. Dhar, P. Schaaf, N. Blic, Y.L. Huang, M. Seibt, and K.P. Lieb, J. Appl. Phys. 90, 4474 (2001).
- [14] Y.V. Kudryavtsev, Y.P. Lee, J. Dubowik, Szymanski, and J.Y. Rhee, Phys. Rev. B 65, 104417 (2002).
- [15] J.P. Biersack, J.F. Ziegler, The Stopping and Range of Ions in Solids, Pergamon, New York, 1985.
- [16] L.R. Doolittle, Nucl. Instr. and Meth. B 9, 344(1985).
- [17] K. Lefki, P. Muret, E. Bustarret, N. Boutarek, R. Madar, J. Chevrier, J. Derrien and M. Brunel, Solid State Communications 80, 791 (1991).
- [18] D. H. Tassis, C. A. Dimitriadis, S. Bouladakis, J. Arvanitidis, S. Ves, S. Kokkou, O. Valassiades, S. Logothetidis, and P. Pouloupoulos, Thin Solid Films 310, 115 (1997).
- [19] H. Kakemoto, Y.Makita, S. Sakuragi, and T. Tsukamoto, Jpn. J. Appl. Phys. 38, 5192 (1999).
- [20] R. Sauer, J. Weber and J. Stolz, Appl. Phys. A : Mater. Sci. Process. 36, 1(1985).
- [21] Y. Gao, S. P. Wong, W. Y. Cheung, G. Shao and K. P. Homewood, Appl. Phys. Lett. 83, 42(2003).